Effect of Cloisite 15A Clay Dispersion on the Structural Characteristics of PVDF Nanocomposite Membrane

N. M. Mokhtar[a,b*], R. Naim[c], N. H. Ismail[d]

[a]Faculty of Civil Engineering Technology, Universiti Malaysia Pahang, Lebuhraya Persiaran Tun Khalil Yaakob, 26300 Kuantan, Pahang, Malaysia
[b]Bioaromatic Research Centre, Universiti Malaysia Pahang, Lebuhraya Persiaran Tun Khalil Yaakob, 26300 Kuantan, Pahang, Malaysia
[c]Faculty of Chemical and Process Engineering Technology, Universiti Malaysia Pahang, Lebuhraya Persiaran Tun Khalil Yaakob, 26300 Kuantan, Pahang, Malaysia
[d]Advanced Membrane Technology Research Centre (AMTEC), Universiti Teknologi Malaysia, 81310 UTM Johor Bahru, Johor, Malaysia

ABSTRACT

Recent interest in nanoparticles-reinforced polymer matrices has surged due to their superior properties over virgin polymers. Nevertheless, there remains a gap in research regarding the impact of clay dispersion on polymeric membranes employed in membrane distillation (MD). This study aims to investigate how the dispersion of Cloisite 15A (C15A) clay influences the structure of polyvinylidene fluoride (PVDF) membranes and improves dye removal efficiency. A nanocomposite membrane consisting of polyvinylidene fluoride-Cloisite 15A clay (PVDF-C15A) was prepared using a phase-inversion process. Additionally, a PVDF membrane without clay was prepared as a control. The influence of clay on the crystalline structure of the PVDF membrane was examined by analyzing morphology, porosity, wetting pressure, contact angle, surface roughness, mechanical strength, and thermal stability. X-ray diffraction spectroscopy and transmission electron microscopy were employed to assess the dispersion state of the clay. The fabricated membranes were evaluated in direct contact membrane distillation for treating dyeing solution. To understand the interaction between dye particles and the membranes, zeta potentials of both the control and nanocomposite membranes were measured. The study revealed that the nanocomposite membrane exhibited higher permeate flux compared to the control membrane. This improvement was primarily attributed to the well-dispersed layered silicate within the nanocomposite membrane, which enhanced its structural properties significantly.

Keywords: Polyvinylidene fluoride, clay dispersion, nanocomposite, membrane distillation, dyeing wastewater

1.0 INTRODUCTION

Membrane distillation (MD) is a heat-driven separation process that transports vapor molecules across a porous hydrophobic membrane [1]. Temperature changes across the membrane generate a difference in vapour pressure, which functions as a driving force. Because of its vapor-liquid equilibrium mechanism, MD can result in either a nearly complete separation (near pure components) or a partial separation that increases the concentration of the mixture's selected components. The MD technique offers a very high pollutant rejection rate, possibly approaching 100% [2]. MD

technology, as part of its high removal efficiency, may reduce treatment process operating costs since it requires low operating temperature and pressure and can be compatible with renewable energy sources like as solar energy to supply thermal energy [3].

Polyvinylidene fluoride (PVDF) is a high-performance thermoplastic polymer with a semi-crystalline structure that is the world's second most manufactured fluoropolymer [4]. PVDF has been used in a wide range of industrial and sophisticated applications because to its mechanical reliability, more effective chemical resistance, and high thermal stability (in comparison to other thermoplastics) [5]. In recent decades, polymer-clay nanocomposites have attracted considerable interest among materials scientists and engineers due to their superior properties compared to pure polymers. Bonyadi and Chung were pioneers in this field, focusing on dual-layer hydrophilic-hydrophobic hollow fiber membranes incorporating two distinct types of inorganic fillers: Cloisite Na$^+$ and Cloisite 15A (C15A) [6]. Cloisite Na$^+$, known for its hydrophilic nature, was integrated into polyacrylonitrile (PAN) to formulate the inner dope solution, while Cloisite 15A, with its hydrophobic properties, was blended with PVDF for the outer dope solution. The primary objective of incorporating clay in their research was to reinforce the polymer structure and enhance its mechanical strength.

Edwie *et al.* introduced self-synthesized fluorinated silica particles (FSi) as a hydrophobic modifier in dual-layer hollow fiber membranes [7]. These particles were employed to improve surface hydrophobicity, leading to enhanced flux rates. However, the membranes encountered wetting issues attributed to the hydrophilic hydroxyl groups present on the FSi particles. Subsequently, Prince

et al. studied the development and analysis of PVDF-clay nanomembranes using the electrospinning technique [8]. The nanofibers produced demonstrated superior performance compared to pure PVDF membranes. Specifically, the inclusion of Cloisite 20A clay particles influenced the membrane's crystallization process, thereby increasing its melting point. Moreover, clay incorporation enhanced the membrane's hydrophobicity. To date, no studies have specifically explored the impact of clay dispersion on the structural properties of MD membranes. Therefore, this paper aims to investigate the influence of the dispersion state of C15A clay on the structure of PVDF membranes and its beneficial effects on dye removal using MD.

2.0 MATERIALS AND METHOD

2.1 Materials

Polyvinylidene fluoride polymer (PVDF, Kynar 760) purchased from Arkema Inc., Philadelphia, USA was used as a base polymer. Cloisite 15A clay (C15A) was obtained from Southern Clay Products, Inc. and was used as received. N-methyl-2-pyrrolidone (NMP, >99.5%) (Merck) was used as a solvent and ethylene glycol (EG, ≥99.5%) (Merck) was used as a non-solvent additive in the polymer solution. Reactive black 5 (RB5, M_w = 991g/mol) from Sigma-Aldrich was used to synthesize dye solution by dissolving it in deionized water produced by ELGA Micromeg Deionizer.

2.2 Fabrication of PVDF and PVDF-C15A Hollow Fiber Membranes

The PVDF pellets and C15A powder underwent initial drying in a vacuum

oven overnight at 60±2°C to eliminate moisture. A dope solution without clay powder was prepared to create a control membrane by dissolving 12 wt.% PVDF in 88 wt.% NMP and 8 wt.% EG. Another dope solution was formulated by adding 3 wt.% C15A powder to the control dope solution. The spinning conditions and the spinning procedure are described elsewhere in our previous publication [5].

2.3 Characterization of the Fabricated Membranes

X-ray diffraction (XRD) analysis of both Cloisite 15A powder and the fabricated membranes was conducted using an XRD-X'Pert PRO diffractometer (PANalytical, The Netherlands) equipped with copper Kα radiation ($\lambda = 0.1542$ nm, operated at 35 kV and 35 mA). The diffractograms were recorded at a scanning rate of 2°/min over a 2θ range of 1.5–10° at room temperature. The morphology of the fabricated membranes was examined using a field emission scanning electron microscope (FESEM) (model: SU-8020, Hitachi). The distribution of clay particles within the nanocomposite membrane was analyzed using Transmission Electron Microscopy (TEM) with a LIBRA 120 EFTEM instrument (Carl-Zeiss SMT, Oberkochen, Germany). The membrane surface roughness was assessed using an atomic force microscope (AFM) (Multimode Nanoscope, DI company). The liquid entry pressure (LEP) of the membranes was determined using a standard method described in the literature. Contact angle (CA) measurements were conducted using a CA goniometer (OCA15plus, DataPhysics). The mean pore size, d_p of the fabricated membranes was measured using a PMI capillary flow porometer (Porous Materials Inc., USA), and the membrane porosity (%),

ε, was calculated following the method outlined by Chabot *et al.* [9]. Particle size and zeta potential analyses were performed using a nanoparticle size analyzer equipped with a zeta potential analyzer.

2.4 Performance Testing of the Fabricated Membranes

A stainless-steel module was employed to evaluate the MD performance. Detailed specifications of the module and membranes can be found in in our previous publication [5]. Experiments were conducted at feed temperature of 70°C, with the inlet temperature of the cold stream maintained at a constant 20°C. Temperature control for both streams was achieved using a coiled heater (model 830, PROTECH) and a chiller (model F26-ED, JULABO), respectively. Permeate flux, J of the tested membranes (kg/m^2.h) was determined using Equation (1).

$$J = \frac{\Delta W}{A \Delta t} \qquad (1)$$

where ΔW (kg) is the weight of permeate collected over a predetermined time Δt (h) and A (m^2) is the effective membrane area. Meanwhile, to determine dye rejection, R (%) of the membranes, Equation (2) was employed.

$$R = \left(1 - \frac{C_p}{C_f}\right) \times 100 \qquad (2)$$

where C_p and C_f are the RB5 concentration (g/L) in the bulk permeate and feed solution, respectively. The concentration of the RB5 was measured by a UV-vis spectrophotometer (DR5000, Hach) with absorbance measured at 597 nm which the maximum absorption occurs.

3.0 RESULTS AND DISCUSSION

3.1 Physicochemical Analysis of the Fabricated Membranes

Figure 1 depicts the membrane morphology of both modified and unmodified membranes incorporating C15A. As shown in Figure 1(b)(i), the PVDF-C15A membrane exhibits more pronounced finger-like structures compared to the control membrane. Such narrow finger-like structures are known to be advantageous in reducing mass resistance during vapor transport. The presence of C15A particles on the inner surface of the nanocomposite membranes was clearly observed. In the PVDF–C15A membrane, these particles appeared well-dispersed on the inner surface without significant agglomeration. Conversely, clay particles were distinctly visible on the outer surface of the nanocomposite membrane, contributing to a rougher surface texture compared to the control membrane. Additionally, incorporating C15A increased the CA of the PVDF–C15A membranes, primarily due to the enhanced surface roughness. This phenomenon can be attributed to the Wenzel or Cassie effect, where the presence of air pockets beneath the rough surface impedes liquid penetration into the grooves, thereby enhancing surface hydrophobicity.
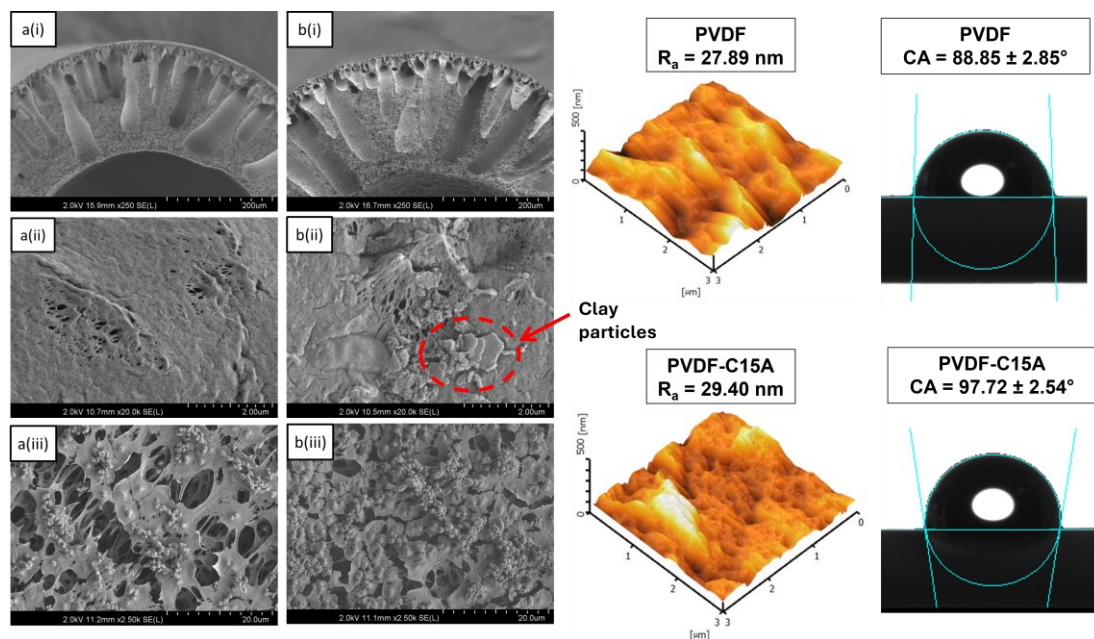
Figure 1 FESEM images of (a) PVDF and (b) PVDF-C15A in (i) cross-section, (ii) outer, and (iii) inner surface of the hollow fiber membranes together with the AFM and CA images

Figure 2 illustrates the XRD analysis results of C15A clay powder, PVDF hollow fiber membrane, and PVDF-C15A hollow fiber membrane. The d001 basal spacing for C15A clay powder was determined to be 1.21 nm (calculated using the Bragg equation). Notably, no distinct peak corresponding to C15A was observed in the XRD patterns of the nanocomposite membrane, suggesting that the C15A minerals were exfoliated and effectively dispersed within the PVDF matrix. According to Villaluenga et al., exfoliation occurs when the diffraction peak (d_{001}) associated with the clay layers is no longer discernible in the XRD analysis [10]. This indicates that

the clay layers have been fully separated, with individual layers uniformly distributed throughout the polymer matrix. To further confirm the dispersion of clay within the PVDF membrane matrix, Table 1 presents the quantitative EDX analysis of PVDF and PVDF-C15A membranes. The presence of C15A in the membrane matrix is confirmed by the detection of silicon (Si), aluminium (Al), and oxygen (O) on the PVDF-C15A membrane.
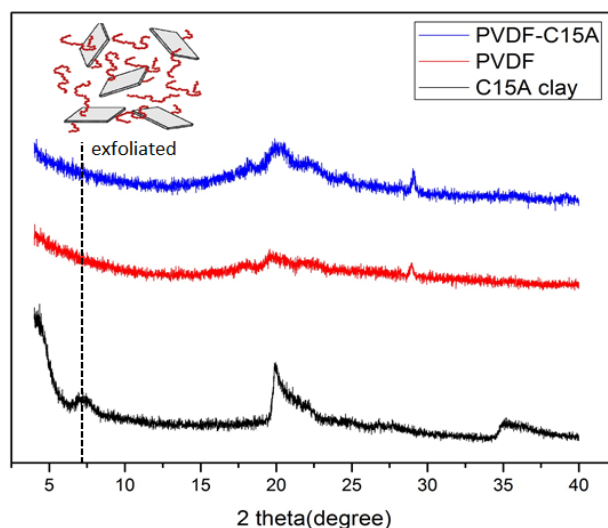
Figure 2 XRD diffractograms for the C15A powder, PVDF and PVDF–C15A hollow fiber membranes

Table 1 EDX quantitative analysis of PVDF and PVDF-C15A composite membranes

Membrane	F	C	O	Si	Al
PVDF (inner layer)	58.44	41.56	-	-	-
PVDF (outer layer)	56.84	43.16	-	-	-
PVDF-C15A (inner layer)	56.18	39.80	3.62	0.26	0.14
PVDF-C15A (outer layer)	54.47	40.68	4.30	0.38	0.17

Furthermore, TEM was utilized to examine the exfoliation state of C15A clay in the nanocomposite membrane (as shown in Figure 3). The stacked silicate layers of C15A clay, consisting of parallel individual layers, are clearly visible and dispersed randomly throughout the matrix. There are two types of exfoliation processes: partial exfoliation and full exfoliation. Partial exfoliation occurs when clay particles maintain an ordered orientation with packed silicate layers, indicating infiltration of PVDF polymers into the structured clay layers. In contrast, full exfoliation occurs when the silicate layers are completely delaminated into individual plates and finely dispersed within the polymer network. External stresses exerted by the polymer chains during mixing can induce the slippage of clay layers, leading to their dispersal in various directions. As depicted in Figure 3, the darker regions represent stacked clay silicate platelets that exhibit partial exfoliation characteristics, where some degree of orientation is observed. Conversely, less oriented and randomly dispersed individual clay silicate platelets can be observed in other areas of the membrane.

Table 2 compiles key membrane properties crucial for the MD process. It

is evident that incorporating C15A particles markedly enhanced membrane characteristics such as wetting pressure, hydrophobicity, and mean pore size. This improvement suggests that the presence of clay particles in the membrane matrix has disrupted the arrangement of polymer chain packing, thereby enhancing structural integrity. The higher LEP values observed with the nanocomposite membranes indicate their ability to resist liquid penetration through membrane pores, which can occur due to variations in pressure between the feed and permeate sides. The impact of incorporating C15A on membrane porosity was found to be negligible in this investigation, as all membranes exhibited relatively high porosity (>82%). It is therefore attributed that the high porosity of the membranes resulted primarily from the low polymer concentration used and the contribution of EG. Thermal analysis revealed a slight increase in the melting temperature (T_m) of the nanocomposite membranes, rising to 169.85 °C from 164.54 °C observed in the control membrane. This suggests that the presence of clay particles may influence the crystallization process of the PVDF–C15A membrane and the flexibility of polymer chains. Moreover, the addition of C15A resulted in a 14% increase in the mechanical strength of the nanocomposite membrane. These findings align well with previous studies [6-8].
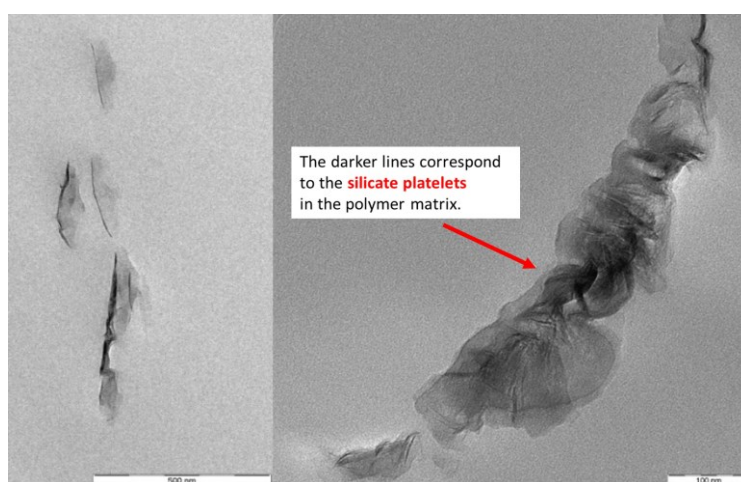
Figure 3 TEM images of the PVDF-C15A hollow fiber membrane

Table 2 Characteristics of PVDF hollow fiber membrane

Membrane Characteristic	LEP (psi)	ε (%)	d_p (µm)	T_m (°C)	Tensile strength (Mpa)	Zeta potential charge (MeV)
PVDF	2.90	82.74 ± 0.66	0.0444	164.54	7.48 ± 0.72	-2.5
PVDF-C15A	13.05	83.70 ± 0.67	0.0880	169.85	8.54 ± 0.58	-4.8

3.2 Performance Evaluation of the Fabricated Membranes

Figure 4 illustrates the permeate flux and dye rejection of PVDF and PVDF-C15A hollow fiber membranes using a feed solution containing 0.05 g/L RB5 dye. In this study, only water vapor can

permeate through the pores from the feed side, while dye molecules are retained and recycled back to the feed tank. The transport of water vapor follows the principle of vapor/liquid equilibrium (VLE), where both heat and mass transfer occur simultaneously across the membrane [11]. The PVDF-C15A membrane consistently achieved a flux of approximately 10.1 kg/m^2.h, representing nearly a 70% increase compared to the control PVDF membrane. This enhancement can be attributed to the PVDF-C15A membrane's higher LEP and CA values, indicating its superior ability to resist liquid intrusion into the membrane pores [8]. Furthermore, this membrane exhibits the smaller mean pore size, which reduces its susceptibility to wetting. Regarding dye removal, PVDF-C15A consistently exhibited high separation efficiency with an average dye rejection rate of 99.9%. In contrast, the performance of the PVDF membrane showed a slight decline over the testing period. The consistent performance of the PVDF-C15A membrane can be attributed to its structural properties. Additionally, the membrane's higher negative charge likely contributed to enhanced dye rejection by repelling the negatively charged RB5 dye molecules, which contain sulphonate groups (SO^{3-}) [12].
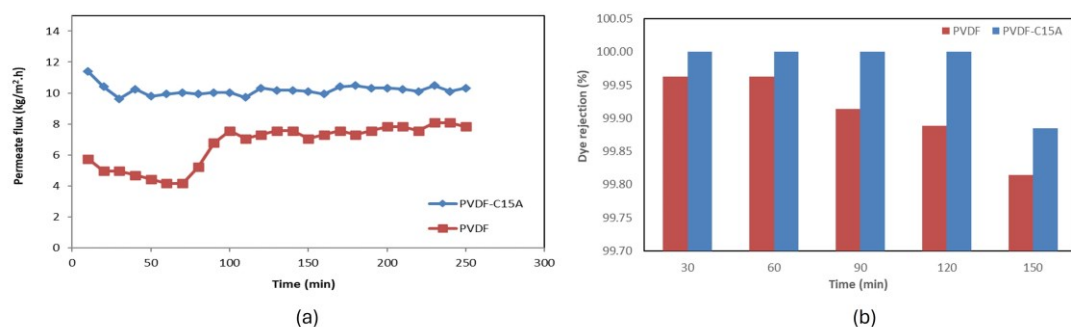
Figure 4 (a) Permeate flux and (b) dye rejection of the membranes after testing using RB5 dyeing solution

Figure 5 illustrates the permeate flux of the PVDF-C15A hollow fiber membrane during the treatment of 0.05 g/L RB5 for up to 480 minutes under fixed conditions of 70ºC and 20ºC for the feed and permeate temperatures, respectively. Initially, the permeate flux of the MD process was recorded at approximately 11.40 kg/m²·h, but it slightly decreased to 10.14 ± 0.26 kg/m²·h throughout the testing period. The PVDF-C15A membranes maintained excellent RB5 rejection, achieving a removal rate of over 99%. For comparison, Table 3 provides an overview of previous MD studies using clay nanocomposite membranes. It is clear that the performance of our membrane is on par with, or even surpasses, that of other nanocomposite membranes. This also highlights that the inclusion of clay improves the MD process by enhancing membrane properties.
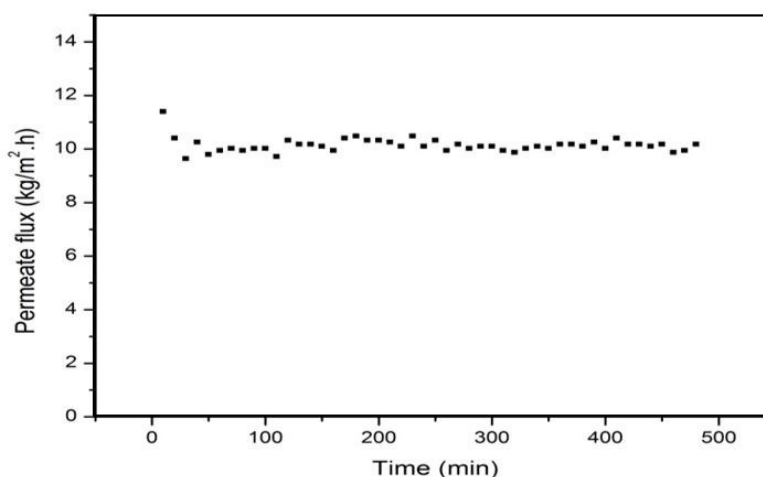
Figure 5 Long-term study of the PVDF-C15A membranes after testing using RB5 dyeing solution.

Table 3 Performance comparison of MD applications that incorporate clay as additive/filler in membrane

Application	MD configuration	Membrane with additive/ filler	Performance	Reference
Rubber processing wastewater	DCMD	PVDF-Cloisite® 15A hollow fiber membrane	96% removal efficiency irrespective of water contaminant parameters.	[13]
Desalination	AGMD	Alumina-Kaolin capillary membrane	Maximum flux obtained was 4.11 L/m².h with salt rejection of 99.96%.	[14]
Arsenic wastewater	DCMD	Polyethersulfone (PES)-Kaolin hollow fiber membrane	100% arsenic removal.	[15]
Oil palm wastewater	DCMD	PVDF-Bentonite hollow fiber membrane	Maximum flux of 5.2 kg/m².h with more than 99% rejection of color, chemical oxygen demand and tubidity.	[16]
Desalination	AGMD	PVDF-Cloisite® 20A Flat sheet membrane	Maximum flux of 8.6 kg/m².h with salt rejection of 99.8%	[17]
Dyeing solution	DCMD	PVDF-Cloisite® 15A hollow fiber membrane	Maximum flux obtained was 10.1 kg/m².h with dye rejection of 99.9%.	This study

4.0 FUTURE RECOMMENDATIONS

The PVDF-C15A membranes demonstrate significant potential for improving the separation efficiency of conventional MD processes. Therefore, it is recommended to integrate these membranes with renewable energy technologies, such as solar-powered membrane distillation (SPMD) systems. By combining renewable energy with advanced membrane technology, SPMD offers a sustainable, cost-effective, and scalable solution to address global water scarcity [18]. The composite structure of PVDF-C15A enhances its hydrophobicity, which helps mitigate common challenges in MD systems, such as membrane wetting and fouling. This increased hydrophobicity, along with the membrane's high permeability, facilitates efficient water vapor transport while minimizing the risk of liquid intrusion, thus improving separation performance. Furthermore, the inclusion of Cloisite 15A

nanoparticles bolsters the membrane's mechanical strength, thermal stability, and anti-fouling properties, resulting in enhanced long-term performance, reduced maintenance needs, and an extended operational lifespan in SPMD systems.

Additionally, PVDF-C15A membranes can optimize solar energy utilization in MD by improving heat retention and maintaining the necessary temperature gradient for effective water evaporation. Their ability to retain heat and facilitate efficient mass transfer is particularly beneficial in solar wastewater treatment systems, where maximizing solar energy input is key to improving permeate flux. As a result, integrating PVDF-C15A membranes in SPMD systems could provide a more cost-effective, sustainable solution for freshwater production, addressing both energy and water challenges in remote or arid areas. This approach not only aligns with the growing demand for green technologies but also supports several of the United Nations' Sustainable Development Goals (SDGs), particularly those related to clean water and sanitation (SDG 6), affordable and clean energy (SDG 7), and climate action (SDG 13).

5.0 CONCLUSION

The C15A clay particles demonstrated excellent compatibility and were uniformly dispersed within the polymer matrix. XRD and TEM analyses confirmed successful exfoliation of the layered silicate clay in the PVDF membrane matrix. The incorporation of C15A resulted in notable improvements in various structural properties such as LEP, CA, surface roughness, tensile strength, and melting temperature of the membranes. During DCMD experiments using dyeing solutions, the PVDF-C15A membrane achieved a permeate flux of approximately 10 $kg/m^2.h$, completely free of dye molecules. In conclusion, integrating C15A into PVDF membranes not only enhances their structural properties but also improves their performance in the membrane distillation process.

CONFLICTS OF INTEREST

The authors declare that there is no conflict of interest regarding the publication of this paper.

REFERENCES

[1] S. Yang, Saade A. Jasim, D. Bokov, S. Chupradit, A. T. Nakhjiri, A. S. El-Shafay. (2022). Membrane distillation technology for molecular separation: A review on the fouling, wetting and transport phenomena. *J. Mol. Liq., 349*, 118115.

[2] J. Li, D. Wang, J. Zhang, N. Zhang, Y. Chen, Z. Wang. (2023). High performance membrane distillation membranes with thermo-responsive self-cleaning capacities. *Desalination, 555,* 116544.

[3] M. A. H. M. Hanoin, F. N. Zainuddin, N. M. Mokhtar. (2022). A Review of Solar-Powered Membrane Distillation System: Concept Design and Development. *The Eurasia Proceedings of Science Technology Engineering and Mathematics, 21,* 27–38.

[4] R. Dallaev, T. Pisarenko, D. Sobola, D., F. Orudzhev, S. Ramazanov, T. Trčka. (2022). Brief review of PVDF properties and applications potential. *Polymers, 14,* 4793.

[5] N. M. Mokhtar, W. J. Lau, B. C. Ng, A. F. Ismail. (2014). Physicochemical study of polyvinylidenefluoride–Cloisite15A® composite membranes for membrane distillation application. *RSC Advances, 4,* 63367–63379.

[6] S. Bonyadi, S., T. S. Chung. (2007). Flux enhancement in membrane distillation by fabrication of dual layer hydrophilic–hydrophobic hollow fiber membranes. *J. Membr. Sci., 306,* 134–146.

[7] F. Edwie, M. M. Teoh, T. S. Chung. (2012). Effects of additives on dual-layer hydrophobic–hydrophilic PVDF hollow fiber membranes for membrane distillation and continuous performance. *Chem. Eng. Sci., 68,* 567–578.

[8] J. A. Prince, G. Singh, D, Rana, T. Matsuura, V. Anbharasi, T. S. Shanmugasundaram. (2012). Preparation and characterization of highly hydrophobic poly(vinylidene fluoride) – Clay nanocomposite nanofiber membranes (PVDF–clay NNMs) for desalination using direct contact membrane distillation. *J. Membr. Sci.,* 397–398, 80–86.

[9] S. Chabot, C. Roy, G. Chowdhury, T. Matsuura. (1997). Development of poly(vinylidene fluoride) hollow-fiber membranes for the treatment of water/organic vapor mixtures. *J. Appl. Polym. Sci., 65,* 1263–1270.

[10] J. P. G. Villaluenga, M. Khayet, M. A. López-Manchado, J. L. Valentin, B. Seoane, J. I. Mengual. (2007). Gas transport properties of polypropylene/clay composite membranes. *Eur. Polym. J., 43,* 1132–1143.

[11] A. Alkhudhiri, N. Darwish and N. Hilal. (2012). Membrane distillation: A comprehensive review. *Desalination,* 287, 2–18.

[12] S. Netpradit, P. Thiravetyan, S. Towprayoon. (2004). Adsorption of three azo reactive dyes by metal hydroxide sludge: effect of temperature, pH, and electrolytes. *J. Colloid Interface Sci., 270,* 255–261.

[13] N. M. Mokhtar, W. J. Lau, A. F. Ismail, D. Veerasamy. (2015). Membrane distillation technology for treatment of wastewater from rubber industry in Malaysia. *Proc. CIRP, 26,* 792–796.

[14] R. Das, K. Sondhi, S. Majumdar, S., S. Sarkar. (2016). Development of hydrophobic clay–alumina based capillary membrane for desalination of brine by membrane distillation. *J. Asian Ceram. Soc., 4*(3), 243–251.

[15] S. K. Hubadillah, M. H. D. Othman, A. F. Ismail, M. A. Rahman, J. Jaafar. (2018). A low cost hydrophobic kaolin hollow fiber membrane (h-KHFM) for arsenic removal from aqueous solution via direct contact membrane distillation. *Sep. Purif. Technol.,* 214, 31–39.

[16] N. A. S. Muhamad, N. M. Mokhtar, R. Naim, W. J. Lau, N. F. Ismail. (2024). Treatment of wastewater from oil palm industry in Malaysia using polyvinylidene fluoride-bentonite hollow fiber membranes via membrane distillation system. *Environ. Pol., 361,* 124739.

[17] R. Navarro-Tovar, P. Gorgojo, M. Jobson, P. Martin, M. Perez-Page.

2024. Innovations in water desalination: enhancing air gap membrane distillation performance by the incorporation of clay nanoparticles into PVDF matrix membranes. *Environ. Sci.: Water Res. Technol., 10*, 2418–2431.

[18] M. A. H. M., Hanoin, F. N. Zainuddin, N. M. Mokhtar. (2022). A review of solar-powered membrane distillation system: *Concept Design and Development, The Eurasia Proc. Sci. Technol. Eng. Math., 21*, 27–38.